Introduction

Cryopreservation

The need for technologies which inhibit or stop ice crystal growth is crucial in modern science, particularly in the field of cryopreservation. Cryopreservation typically involves rapid freezing of, for example, tissues or organs for transplants such that they are cooled down before ice crystal growth can begin. However, these methods typically involve the use of large amounts of cryopreservative which is expensive and simply not viable on a mass scale[1]. There is also the issue of the cytotoxicity of the solvents typically used: preserved cells can lose membrane integrity and have decreases in viability. Dimethylsulfoxide (DMSO) is an example of solvent often used for cryopreservation and recent research has shown that it is cytotoxic[2].

Other methods can be employed to work around these problems, namely the use of additives in cells/tissues to work as antifreezes such that ice crystal growth can be inhibited or even stopped. Through the use of Better additives improvements in long term viability of human tissues/ organs could extend the life of transplants without fears of tissue degradation and far more cost effectively (typically a transplant can be stored for 1 to 3 days before showing losses of viability)[3].

The same uses can be employed in the food industry. Typically frozen food is rapidly cooled down using nitrogen by using additives could allow for more cost effective cryostorage solutions. Ice creams contain a lot of fat but this is simply to stop ice crystals from growing in the cream as its being frozen. If certain additives could be added to stop this, this could allow for a whole new market of low fat ice creams.

Antifreezes in Nature

Biological antifreezes were first discovered in the 1960s[4] in the blood of polar fish species[5]. They have also since been found in a number of other organisms which inhabit sub-zero environments, including a number of insect, plants[6] and fungi. Combined with elevated sugar/ salt concentration, these biological antifreezes allow organism to thrive at temperatures as low as -1.9C[7]. The structures of these antifreezes vary across organisms but they all fill the same role – to prevent cellular damage from ice growth. They are believed to be able to do this by

using some of the specific functional groups to bind to the ice lattice[8] via hydrogen bonds, in turn shaping the way the ice lattice grows around it and neighbouring antifreeze molecules[9].

These biological antifreezes can characterised into 2 types of protein: Antifreeze proteins and antifreeze glycoproteins[10]. Both are made up of amino acid chains with antifreeze proteins having very defined primary, secondary and tertiary structures with a mix or just purely alpha-helices and beta-pleated sheets, but the glycoproteins also have carbohydrate chains attached to the repeat units. The structure of AFGPs has been found to be primarily made of a tri-peptide repeat unit: alanine-alanine-threonine with a disaccharide glycosylated to the threonine residue[11]. The AFGPs consist of between 4 to 50 tripeptide repeat units, and the larger AFGPs have typically shown better ice recrystallization inhibition activity.

The activity of an antifreeze can be characterised by 3 inherent effects:

1. Thermal Hysteresis
2. Dynamic Ice shaping
3. Recrystallization inhibition

Thermal Hysteresis

This describes how the freezing point of a solution is lowered below its natural freezing temperature, beyond the usual colligative effects of addition of a solute[12]. This is a thermodynamic effect where the Gibbs free energies of melting and freezing are lowered in proportion to the concentration of the added solute. The freezing point is reduced to below the melting point of the solution, giving rise to a gap. Within this gap an ice crystal will not melt or grow until the temperature has either increased or decreased out of the temperature range[13].

Dynamic Ice Shaping

This effect is closely related to Thermal hysteresis. The effect is dependent on the concentration of the solute and is believed to be the result of the antifreeze binding directly onto the surface of the ice, via adsorption. The ice then continues to grow in layers around it forming pyramidal structure on the outside of the crystal changing the overall morphology. These lead to the formation of hexagonal pits across the topography of the surface of the ice forming hexagonal bi-pyramidal[14] crystals which, due to their needle like shape, can damage cells by effectively puncturing cell membranes.

Ice Recrystallisation Inhibition

This describes the slowing or complete halting of ice crystal growth. Ice crystal growth is a thermodynamically-driven spontaneous process and is the result of an enthalpically favourable rearrangement of water molecules from small ice crystals to large. For larger ice crystals the surface area to volume ratio is lower and continues to decrease as the crystal grows. This is more favourable for water molecules since more are able to hydrogen bond with the ice lattice, whilst a smaller proportion is exposed to the surface (which is less energetically stable). It is this process, known as Ostwald ripening[16], is most responsible for cell damage.

It is thought that the mechanism for by which biological antifreezes work is by binding to the ice lattice of crystals with site specific groups. Hydroxyl groups are able to act as hydrogen bond donors/acceptors while the hydrophobic backbone of the chain prevents water from reaching the site. The antifreeze acts at the Quasi Liquid layer – a phase boundary approximately 10A in diameter which is neither entirely liquid nor solid but rather lie between them, where molecules become less ordered further away from the ice.

Antifreeze (glyco)proteins' ability to prevent ice growth is thus very desirable and can have many applications in modern medicine and food industries. Their main shortfall however is that their isolation and purification is very time consuming and the required quantities would simply not be feasible. Their dynamic ice shaping properties are another problem in that most tissues or organs would be damaged from the needle-like ice crystal shaping. As mentioned previously, other methods of cryopreservation as possible i.e. with the use of DMSO as a solvent, but problems with cytotoxicity within cells upon thawing out.

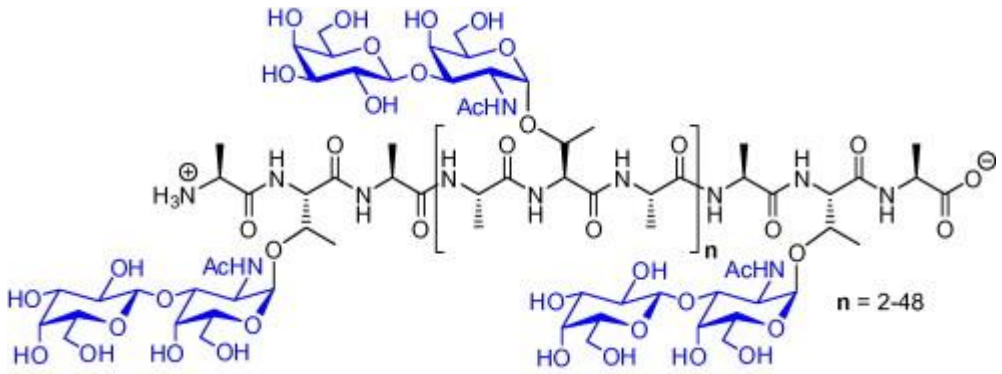

Figure 1 - Structure of a Native Antifreeze GlycoProtein[15]

Antifreeze protein mimics and analogues

Due to the difficulties and expense of extracting and purifying or producing biological antifreezes[17], efforts have been made to go about creating synthetic antifreezes which mimic their ability to inhibit ice growth, for a fraction of the price and time. Synthetic molecules have been produced in the lab based on principles learned from the studying Antifreeze (glyco)proteins. Typically hydroxyl groups are required so that binding to the hydroxyl groups in the ice can take place via the hydrogen bonding. With regard to antifreeze glycoprotein analogues, it was found that removal of the carbohydrate groups or acylation of the hydroxyls resulted in a reduction in activity[18]. Also slight variations in the amino acid backbone haven't been found to affect the activity[18]. These finding seem to indicate that both hydrophilic and hydrophobic groups along with a rigid backbone are required for IRI activity.

Work done by Ben et al. on smaller molecule antifreezes has shown that mono and disaccharides show moderate to low activity in comparison to native AFGPs. They make reference to the hydration ability of sugars and relate it to the carbohydrate groups' ability to modify the structure of the bulk water[19]. The first generation C-linked AFGP analogues by Ben *et al*. showed that an O-linkage is not required for RI activity[21]. These first generation analogues showed a weak RI activity - nearly half the antifreeze activity of native AFGPs[22]. The analogues only had a monosaccharide group rather than the disaccharide, which could explain the reduced activity. They also showed cell viability comparable to that of 2.5 % DMSO solution in thawed cell cultures[20].

The second generation analogues by Ben *et al.* found that the distance between the carbohydrate moiety and the peptide backbone is a key feature, with shorter chains resulting in increases RI potency. Some of their other work Ben *et al.* found that low molecular weight, carbohydrate-based surfactants show moderate activity. They tested n-Octyl-β-D-galactopyranoside for RI activity and found it had markedly higher activity than simple galactose at the same concentration. The glucose variant showed no significant improvement in activity compared to simple glucose or the galactopyranoside. Their work indicates that molecules ability to form micelles, after concentrations go beyond the crtitcal micelle concenctration, is independent of IRI activity.

Interestingly however, polyvinylalcohol (PVA) has been found to show relatively high activity despite not having many of the characteristics expected based on current knowledge. It has a flexible chain made up of several hydroxylated-ethylene monomer repeat units. Work done by Gibson *et al.* has shown that these hydroxyl groups must be present to show activity

without any focus on the backbone, whilst replacement of the hydroxyl with amine groups or carboxylic acid show no activity[7].

Work by Inada et al. has shown the ice inhibition activity of PVA, in a series of splat assays, comparable to that of a type 1 AFP *2003 inada. Increases in the concentration, molecular weight (degree of polymerisation), or the hydrolysis of the PVA, each resulted in better activity. One positive note about PVA is the fact that it is able to show high activity, but at the same time is completely free from toxicity which gives it another reason about it suitability for potential use in cryopreservation.

In contrast, Polyethyleneglycol, which has the same molecular structure of PVA but with a rearrangement such that the oxygen is now o-linked in the backbone, has been found to show little if no activity. Yet it is still readily able to form hydrogen bonds with water and is very soluble in water.

Solid State Nuclear Magnetic Resonance

Nuclear Magnetic Resonance is a technique that is ideal for analysis of nucleic interactions between molecules at an analytical level. Solid state NMR uses the same techniques as solution state NMR but adds additional mechanisms to reduce anisotropic interactions.

Typically methods used to quantify the interactions between antifreezes proteins/ analogous/ mimics have been based upon splat assays using cryomicroscopy and measuring sizes of ice crystals using mean largest grain size calculations. Whilst being able to physically see whether molecules are IRI active and to what extent, it doesn't provide us with quantitative data. NMR also provides a way of gaining data when other methods are simply not feasible due to a number of reasons. Growing single ice crystals, for example, for 1:1 measurements with antifreezes is extremely challenging and time consuming. Using Solid state NMR, we are able to probe interactions between nuclei in the ice and cryprotectant, which allows us to gain some insight into how the water changes behaviour with the addition of a molecule which shows high or low IRI activity.

Nuclei have spin *I* and where *I* is greater than zero, the nuclei contain a magnetic moment. When *I* is a positive integer, the nuclei is said to have an additional quadropolar moment. 1H nuclei have spin a ½ which means they're magnetic and when in the presence of a magnetic field, align themselves in two orientations (nuclei arrange themselves in 2I+1 orientations). These orientations effectively create two populations of nuclei; those with a high energy orientation when aligned against the field and those with a low energy orientation when

aligned with the field. The number of nuclei in each energy state is determined by the Boltzmann distribution:

$$\frac{N_a}{N_b} = e^{\frac{\Delta E}{K_b T}}$$

Where Na and Nb are the population of the nuclei aligned with and against the static magnetic field, respectively, Kb is the Boltzmann constant, T is temperature and ΔE is the energy difference between the two populations. The difference in nuclei between the two states is normally quite small – only 1 in 10,000 for a 1H nuclei in 20T magnet at 298K (or 850MHz). The energy difference between these two levels is given by:

$$\Delta E = \frac{h\gamma B_0}{2\pi}$$

where h is plancks constant, B_0 is the strength of the static magnetic field and Y is the gyromagnetic ratio, which describes the ratio between the magnetic dipole moment to its angular momentum (in effect the strength of the given nucleus' magnet).

One is able to increase sensitivity and resolution for a given nuclei, by increasing the difference in populations. This can be done by increasing the energy difference between the two states, either by increasing the strength of the magnetic field B0 applied (since the gyromagnetic ratio and planck constant remain the same) or lowering the temperature of the sample, as we see from the above equations.

When a radio-frequency pules is applied to the system, nuclei move up from the lower energy state to the higher state, providing the pulse is on resonance. I.e. the oscillation frequency of the pulse applied matches the larmor frequency, ω_0, given by the larmor equation (divided by 2π to convert to Hz):

$$\omega_0 = \gamma B_0$$

The larmour frequency is defined as the angular frequency of precession around the magnetic field, B0 by the nuclei before any pulses are applied.

When a pulse is applied (typically in the x direction) the net magnetisation, initially aligned with the static magnetic field in the Z-axis, nutates perpendicular to the direction of the pulse. The angle of the nutation is dependent are determined by 3 factors:

$$B_1 = Cos(\omega_{rf} t + \theta)$$

Where theta is the flip angle, ω_{rf} oscillating frequency of the pulse and t is the time of the pulse.

A receiver coil is placed in the Y direction, perpendicular to the direction of the radio frequency pulse. After a pulse has been applied, the detector measure signal strongest when the net magnetisation reaches either +Y or –Y directions and has the least signal when the magnetisation reaches +X or –X directions. Once the pulse has been applied, the nuclei relax back to thermal equilibrium via precession across the XY plane until it reaches its initial Z-direction and so the signal decays back to nothing. The signal generated is a free Induction decay and is recorded in a time domain spectrum, which can then be Fourier Transformed into a frequency domain spectrum to give peaks of each of the different environments i.e. the spins that oscillated at slightly different frequencies.

The chemical shift is comprised from the isotropic and anisotropic interactions. In solution state NMR, molecules are able to freely tumble so on the whole anisotropic interactions average out due to Brownian motion i.e. the internuclear vector of nuclei sample all values of theta in a short amount of time. This means high resolution spectra can be obtained to the point where j-couplings can be seen and assigned between different environments. However solids don't have that mechanism to average out these interactions in solid state NMR, which means we get peak broadening and loss of resolution on spectra due to a large amount of dipolar coupling occurring along with chemical shift anisotropy. However, there is a solution to getting high resolution spectra in solid state NMR, and this is by applying magic angle spinning. By spinning a sample around a given axis, the average angular dependence of the anisotropic interactions becomes:

$$\text{Anisotropic interactions} = \frac{1}{2}(Cos^2\theta - 1)$$

Where theta is the angle at which the sample is being spun relative to B0. By tilting the sample relative to B0 such that $Cos^2(\theta) = 0$ (54.7356 degrees), anisotropic interactions are greatly removed, since components perpendicular to the axis of spinning are zeroed from the rotation and at the same time interactions parallel to the spinning axis as zeroed as well due to being tilted at 54.7 degrees. It is common to see spinning side bands on spectra obtained from magic angle spinning solid-state NMR. These will often appear either side of large peaks with a separation equal to the spinning frequency in Hz.

Since the water molecules are frozen in ice, they no longer able tumble freely; hence magic angle spinning is employed for samples run in this project.

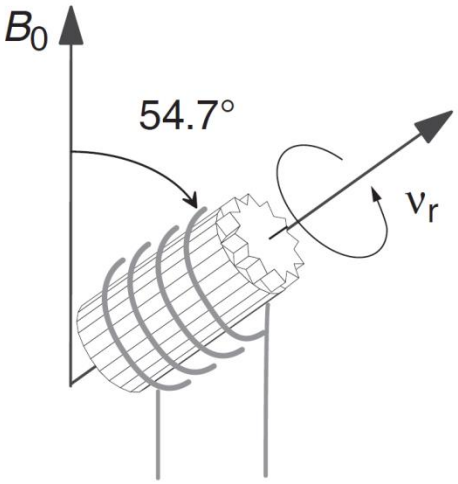

Figure 2 - Diagram illustrating Magic Angle Spinning of a rotor [22]

Relaxation

Relaxation describes the process by which spins return to thermal equilibrium and the decay of any transverse magnetisation. The return of the longitudinal magnetisation to equilibrium is characterised by a spin-lattice relaxation time constant, T1. The decaying of the transverse magnetization is characterised by a spin-spin relaxation time constant, T2.

Small molecular magnetic fields that fluctuate rapidly due to molecular motion induce very small changes in the spins' precession. The most important mechanism of magnetic field fluctuation is the magnetic dipole-dipole interaction between the magnetic moment of two nuclei. This interaction depends not only on the distance between the pair of dipoles but also on their orientation relative to B_0. When a molecule tumbles, the magnitude and direction of the magnetic field one spin is exerting other, changes.

These fluctuations also occur with chemical shift anisotropy. Chemical shifts anisotropy is caused by electrons around the nuclei moving by the current induced by the external magnetic field, B0. As the molecules tumble in a liquid, the direction and the magnitude of these local fields also change. This relaxation mechanism arises whenever the nucleus has a non-spherical electronic environment.

Quadrupolar nuclei (nuclei with spin >1/2) also produce these fluctuations and are by the most dominant relaxation mechanism. A Common quadrupolar nuclei used are deuterium and Nitrogen-14.

If the intramolecular dipole–dipole couplings are the only relaxation mechanism present in a system, the spin–lattice relaxation rate constant, T1, for the two-spin system is given by[24]:

$$\frac{1}{T_1} = \frac{3}{10} b^2 \{\mathcal{J}(\omega^o) + 4\mathcal{J}(2\omega^o)\}$$

where the quantity (ω0) is the spectral density of the dipole–dipole couplings at the Larmor frequency ω0[24]. The spin-spin ralxation constant, T2, is given by:

$$\frac{1}{T_2} = \frac{3}{20} b^2 \{3\mathcal{J}(0) + 5\mathcal{J}(\omega^o) + 2\mathcal{J}(2\omega^o)\}$$

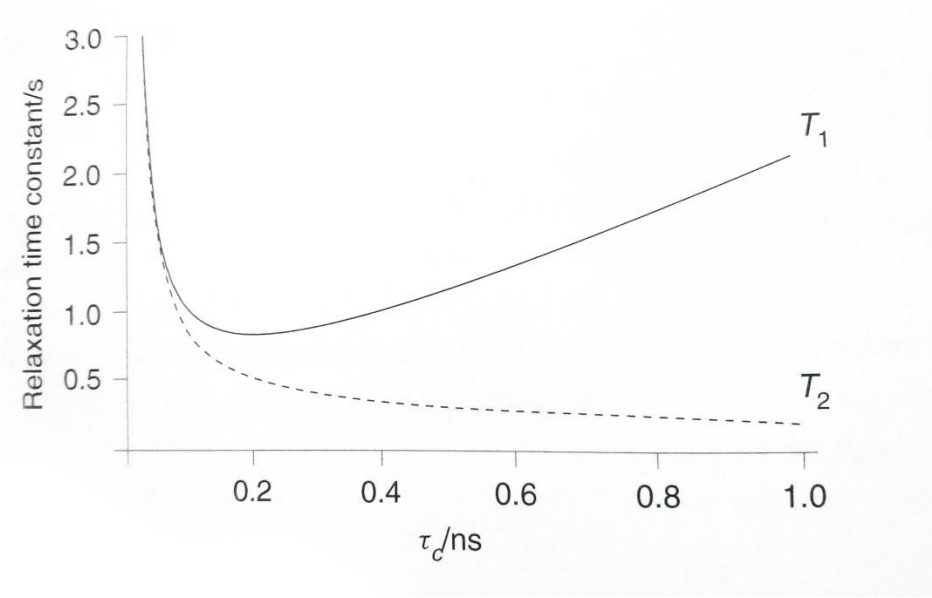

Figure 3 - Variation of T1 and T2 with correlation time, intramolecular dipole-dipole relaxation[24]

The spectral density, in turn, is defined as twice the Fourier transform of the autocorrelation function. Thus, equations correlate the relaxation times *T1* and *T2* with the spectral density, and in turn, with the correlation time[24].

The parameter c is called *correlation time* of the field fluctuation. Rapid fluctuations have a small value of c, while slow fluctuations have a large value of c. The correlation time indicates how long it takes for the random field to change its sign which corresponds to the *rotational correlation time* of the molecules. The rotational correlation is approximately given by the average time taken for the molecules to rotate by one radian[24]. Rotational correlation time is actually dependant on the temperature where the higher the temperature the shorter the rotational correlation time. It is influenced by the viscosity of the liquid, where small molecules in non-viscous liquids will have short times, while larger molecules and viscous liquids will have longer times[24].

T1 and T2 curves are a function of the correlation time. T1 will have minimum at a particular point whilst T2 will decrease with the increasing.

In general, the T1 and T2 relaxation values can tell us a lot about how protons in the water are interacting with the cryo-protectant is interacting, specifically how they are tumbling. Since viscosity plays a large part of relaxation times, it can tell useful information about the ordering of the bulk water when it's frozen and potentially uncover key facts about what the mechanisms cryo-protectants use in their roles and how they interact.

Ben et al. have also tested type III antifreeze proteins in Solid-state NMR. They measured T1 relaxations of 3 different type III proteins in deuterium, that were shown to be IRI active, along with pure D2O and a negative control protein. Differences in the relaxations showed the negative control had times closer to pure D2O whilst the positive controls showed much faster relaxation times. They concluded that these protein don't appear to bind directly to the ice despite showing high IRI activity[27]

Aims

The aims of this project were to take frozen samples of Poly Vinyl Alcohol and Poly Ethylene Glycol dissolved in Phosphate Buffer Saline solution and to run a series of Solid-State NMR experiments on them in order to gain some insight into why these compounds show high ice recrystallization inhibition activity and not, respectively.

A second aim was to compare this data to the splat test assay data collected via a cryomicroscope.

Experimental Methods

Materials

Unless otherwise stated, all chemicals used in any synthesis or experiments were purchased directly from Sigma-Aldrich. Altogether 4 different polymers were used, three PolyvinylAlcohol (PVA) and one PolyEthyleneGlycol (PEG): One PVA with mass of 13kDa and the PVA with a mass of 4.6kDa. The other two PVA polymers, with mass 1kDa and 4.4kDa were synthesised in our lab. Phosphate buffer Saline was made up by dissolving pre-made tablets in 200ml of distilled water.

PolyvinylAlcohol Synthesis

0.055g of S-Benzyl O-ethyl carbonodithioate (RAFT agent), 0.264g of Vinyl Acetate (equivalent of 24 monomer units) and 0.0052g of AIBN (radical initiator) were taken an added to a round bottomed flask and rubber stopped. The solution was then degassed using two needles (intake and outtake through the rubber stopper) for 30 minutes to remove any oxygen since it denatures the RAFT agent. The solution heated in an oil bath at 67C (AIBN activates at 60C and the RAFT agent evaporates at 70C) while being magnetically stirred and left to react overnight. The solution was then taken and peipeeted into a whirlpool of 100ml petroleum ether 40-60C to dissolve any unreacted material and impurities. The solution was then centrifuged in a Eppendorf centrifuge 504R and decanted off. The remaining viscous liquid was dissolved in minimum Tetrahydrofuran, rotary evaporated off and left in a dessicator to dry overnight. A small amount of the dessicated liquid was then transferred to a small vial and dissolved in THF again and then plunged through filter paper to run in Gel permeation Column at 7.45 Bar to test to see the polydispersity index. The remaining liquid was taken and 0.16g of hydrazine (20 equivalents) was added and the solution again heated and stirred for 30 minutes at 67C. The solution was then transferred to a special bag with holes in and filled with milliQ water. The bag was then sealed either side with plastic clips and left to stir in a large beaker also filled milliQ water for 2 days, with replacing of the water occurring every 6 hours. The final solid was then extracted and freeze-dried using a Heto lyolab 300 freeze dryer. This produced the 1kDa PVA.

The same procedure was repeated but with 0.55g S-Benzyl O-ethyl carbonodithioate (RAFT agent), 0.6g of Vinyl Acetate (equivalent of 100 monomer units), 0.0052g of AIBN (radical initiator) and 0.16g of hydrazine, to produce the 4.4kDa PVA.

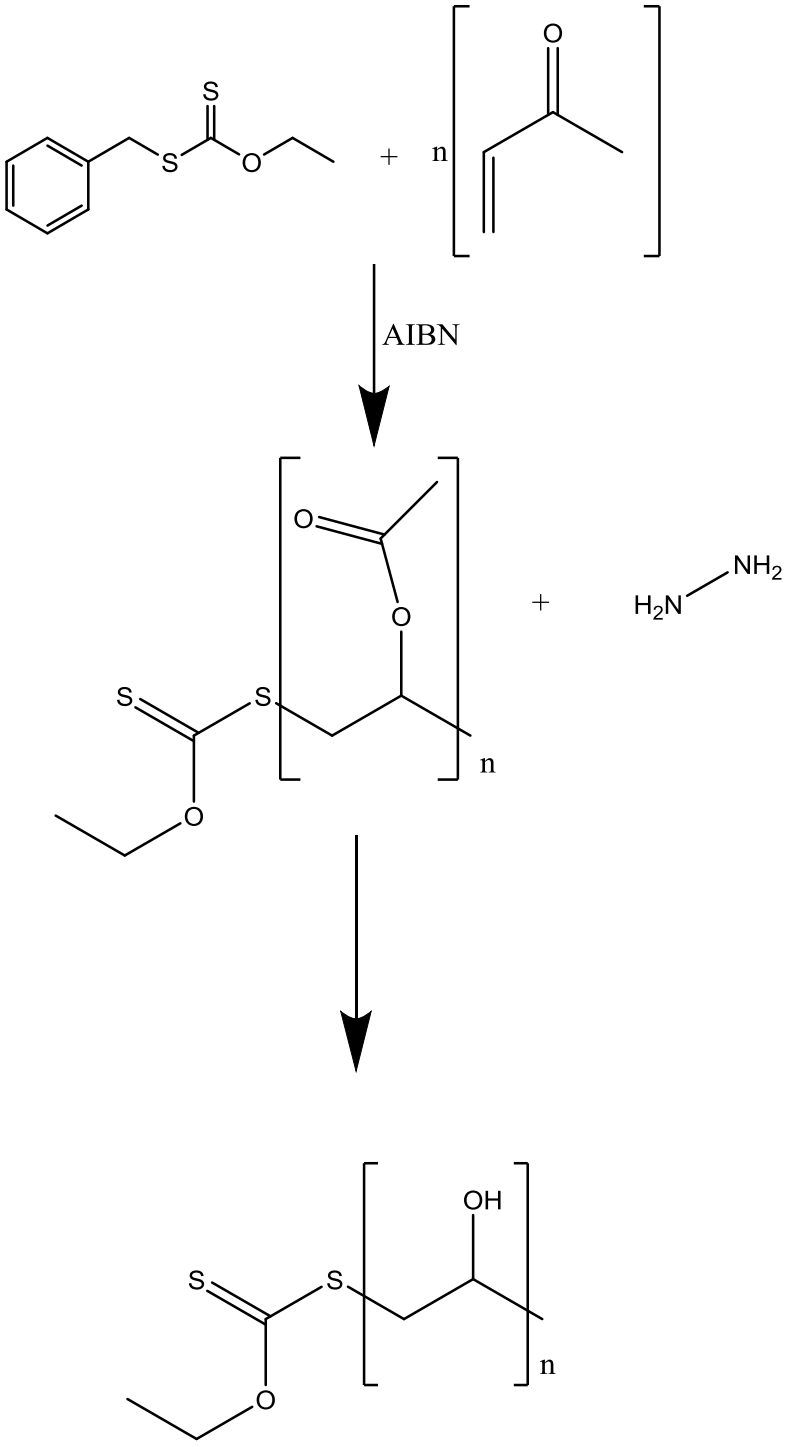

Figure 4 - Synthesis of Poly Vinyl Alcohol by Reversible Addition−Fragmentation chain-Transfer Polymerization of vinyl acetate and the hydrolysis of Poly Vinyl Acetate

Sample preparation

PBS is a salt based water solution containing several different salts including NaCl and KCl. It is used since the phosphate groups help to maintain the pH whilst the salt concentrations match tend to match those found in the body and so is relevant to the field of cryopreservation. Samples were made up by dissolving masses of polymer into volumes of phosphate buffer saline solution (PBS) solution at heated at 70C while being stirred:

Table 1 - The masses of Polymer Dissolved in volumes of PBS to make a series of concentrations of PVA/ PEG in water

Polymer	Mass of polymer added /g	Volumes of PBS added /ml	Concentration / $mgml^{-1}$
PVA 13kDa	0.01	10	1
	0.015	10	1.5
	0.02	10	2
	0.03	10	3
	0.05	10	5
	0.1	10	10
	0.15	10	15

It should be noted that preparation of a 13kDa 20 mg/ml sample was attempted but simply could not fully dissolve and so is not included in the results. Serial dilutions were used for concentrations less that 1 mg/ml for accuracy (minimum weight for scales to be accurate was 0.01g):

Table 2 - The masses of Polymer Dissolved in volumes of PBS to make a series of concentrations of PVA/ PEG in water

Sample	Volume of sample added /ml	Volume of PBS added /ml	Concentration / $mgml^{-1}$
13kDa 0.1 mg/ml	1	9	0.01
13kDa 0.1 mg/ml	1	1	0.05
13kDa 1 mg/ml	1	9	0.1
13kDa 1 mg/ml	1	1	0.5

Similarly, 0.1, 1, 2, 3 mgml samples of 1kDa and 4.4kDa PVA were made using the same procedure of weighing masses and dissolved in PBS solution in vials.

PEG control samples were made up in a similar way but did not require any heating since it is very soluble. 0.5, 1, 2.5, 5, 10, 20 mg/ml concentrations were made up.

Splat Test Assay

A glass syringe was attached to a clamp stand and elevated 2m above a flat aluminium plate cooled by a bed of dry ice. A clean needle was then attached to the syringe and a few drops of samples. A microscope slide was then placed on the metal plate on the trajectory of the syringe. A single drop of sample was then dropped on to it causing it to freeze instantly into a flattened disc (any unused sample was replaced back into the sample vial). The slide was then immediately taken with some tweezers and placed into a Linkam Biological Cryostage BCS196 with a T95-Linkpad system controller and LNP95-Liquid nitrogen cooling pump, and sealed into the stage. The temperature of the stage is was preset to -8C before dropping (Linksys 32 software was used to control the temperature). The slide was viewed using an Olympus CX 41 microscope with lenses x4, x10 and x20 and a picture was then taken with a Canon EOS 500D attached to the top of the microscope at 20x magnification after focussing. Pictures were taken at 0 minutes and then at 30 minute intervals up to 2 hours (as the vessel holding nitrogen ran out beyond this). The pictures were then later processed using open source ImageJ software and Microsoft Excel. This was repeated for a number of different concentrations of the prepared polymer samples.

NMR Experiments

All experiments were performed on a Bruker Avance Ultrashield 500Mhz Spectrometer, using a triple channel HXY 4mm probe while spinning at 5000Hz using a Bruker MAS II. The software used to control the spectrometer was topspin 2.1. Samples were loaded into 4mm rotors using eppendorf autopipettes. All experiments took place at 8C – samples were loaded into the spectrometer, spun at 5000Hz, cooled down to -20C and held there for 5 minutes to allow the sample to freeze, then brought back to -8C. After the probe had been tuned at -8C, experiments were started.

Before experiments could take place, however, the powers had to be optimised, by running a “popt” program. This basically optimised the spectromter such that one could work out what the correct time of the pulse was needed to for the magnetisation to 90 and 180 degrees for a

given power level in dB. At a power level of 8.2dB, the p1 and p2 (90 and 180 degree pulses) were 4.25 and 8.5 us respectively.

Temperature calibration

It should be mentioned that, an external temperature calibration had to be done in order to know what the correct of the sample was. There is normally a small discrepancy between what temperature the sample is and what the probe detects is the correct temperature. The temperature calibration was performed using lead nitrate (PbNO3) using the method outlined by Bielecki and Burum*. Lead nitrate has a unique characteristic by which it changes chemical shift rather significantly with temperature, so as the temperature drops so does the chemical shift in proportion. The sample was loaded into a rotor and spun in the spectrometer. A 1D spectra via 90 degree pulse was then obtained. After doing so, the chemical shift of the characteristic peak for 207Pb was noted down at 10 different temperatures with the target temperature in the range (-8C). A linear relationship between the chemical shift and temperature was then plotted and equation of the line was used to backtrack the correct temperature needed on the probe to reach the actual target temperature, using the difference between calibrated and measured chemical shifts. This was found to be -8.8C and so all experiments were carried out such that the probe read the sample temperature as -8.8C.

Relaxation experiments

Inititally for a sample, a 1D spectrum was recorded first with a 90 degree pulse was measured followed by a measurement of the Spin-lattice relaxation time (T1) followed in turn by a spin-spin relaxation time (T2) measurement. These experiments were then continually run one after the other over a 2 hour period such that they could be compared to the splat test assays run – direct comparison of relaxation times to ice crystal growth as a function of time. However, due to a lack of anything compelling to take away from the data (see discussion) due to a similar relaxation time from each of the experiments throughout the 2 hours, a change was made to run a multitude of different samples in order to see a general trend.

Each of the samples prepared (see above) were then each taken and in turn a T1 and T2 measurement was performed after freezing at -20C and being annealed at -8C.
The T1 relaxtion times were measured using an inversion recovery pulse sequence.
The time t was varied using a variable delay list from 150 ms to 1.5 seconds at 150ms intervals with a relaxation delay of 2 seconds to allow the spins to fully relax. The numbers of scans were set to 8 to allow for good signal: noise.

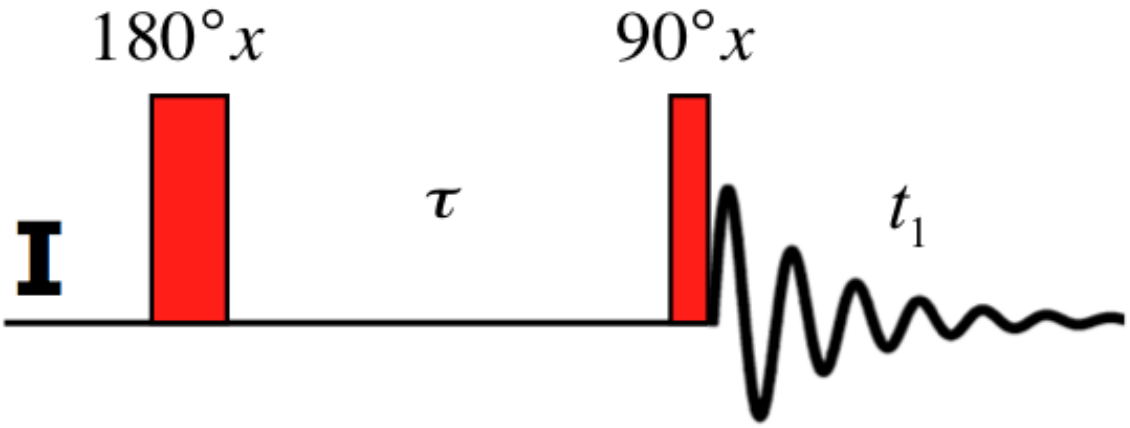

Figure 6 - Diagram of the Inversion Recovery Pulse Sequence

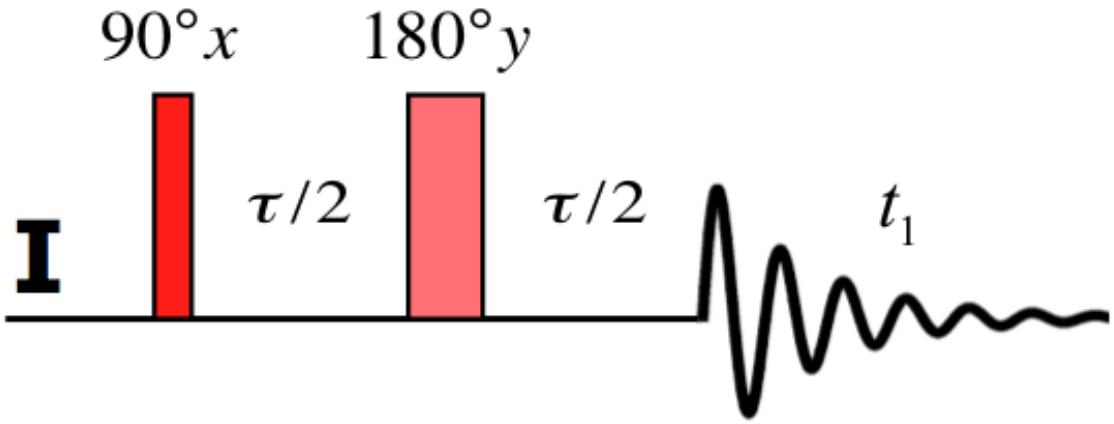

Figure 5 - Diagram of the CPMG Pulse Sequence

T2 relaxation time was measured using a CPMG (abbreviated from Carr, Purcell, Meiboom and Gill) pulse sequence.

The initial 90 degree pulse was 4.25us and the number of loops was controlled by a variable counter list which set the loop counter to 301 starting from 1 and going up in 30 loop intervals. 1 loop consists of a delay (τ/2), a 180 degree pulse and another delay and in this case totalled 0.0020085s (where τ/2 was 0.001 and the 180 degree pulse was 8.5 us). Again the number of scans was set 8 to allow for good signal: noise.

After data was extracted from the spectra – specifically the data points of times against NMR signal intensity, the data was pulled into Origin and fitted using the following functions to give the final relaxation values for each given sample:

$$T1: y = A_1\left(1 - 2e^{\frac{-x}{T_1}}\right) + y_0 \; and \; T2: y = A_1 e^{\frac{-x}{T_2}} + y_0$$

This was done all data obtained from T1 and T2 experiments.

Results and Discussion

Splat test Assays

After taking pictures at timed intervals of 30 mins over a 2 hour period, they were then taken and processed using imageJ to find the Mean largest Grain size of the ice crystals. This basically involved using the measuring tool in imageJ to measure the largest distances across the biggest crystals visible on the picture. These were then tabulated in excel and where the numbers were converted from pixels into um using a reference image in which the shapes' diameter was equal to 100 um. The Mean Largest grain sizes of different concentrations of polymers were then plotted as a function of time (this includes pure PBS to show the comparison).

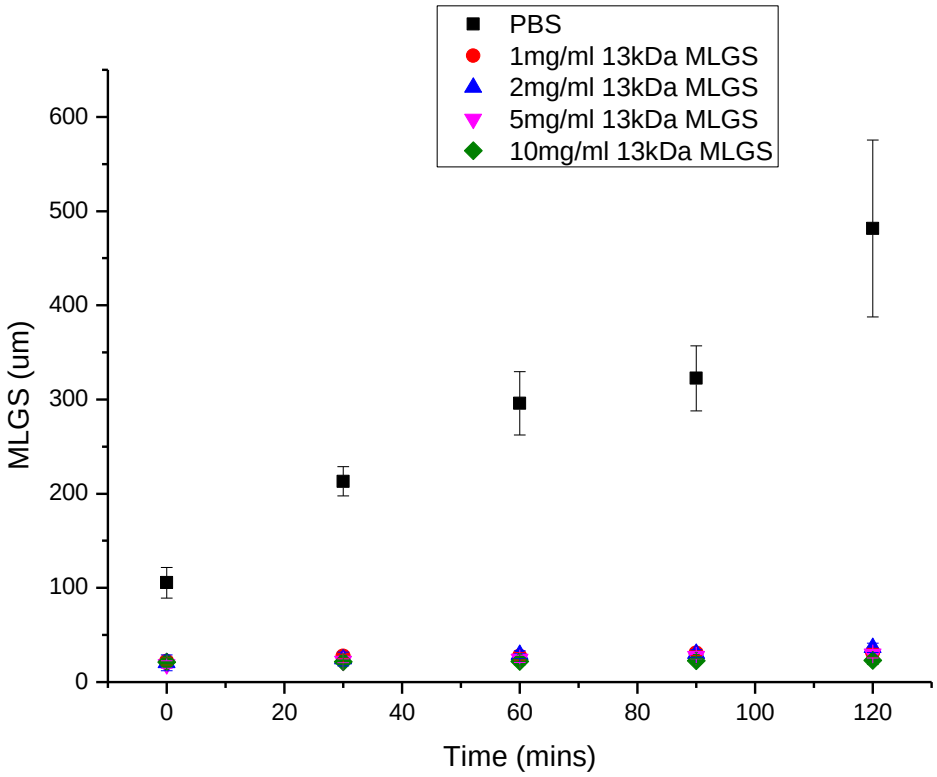

Figure 7 - A plot of Mean Largest Grain Size of Ice crystal against time

As we see immediately, each of the concentrations are very effective as inhibiting the growth of ice. From the PBS assay we see the ice crystal continue to grow to nearly 500 um while the PVA samples hardly go beyond 50 um. This is a clear example that shows PVA shows high IRI activity. Figure 8, shows more clearly the activity of the individual PVA concentrations. On the whole we see, the higher the concentration of polymer in solution, the more ice growth

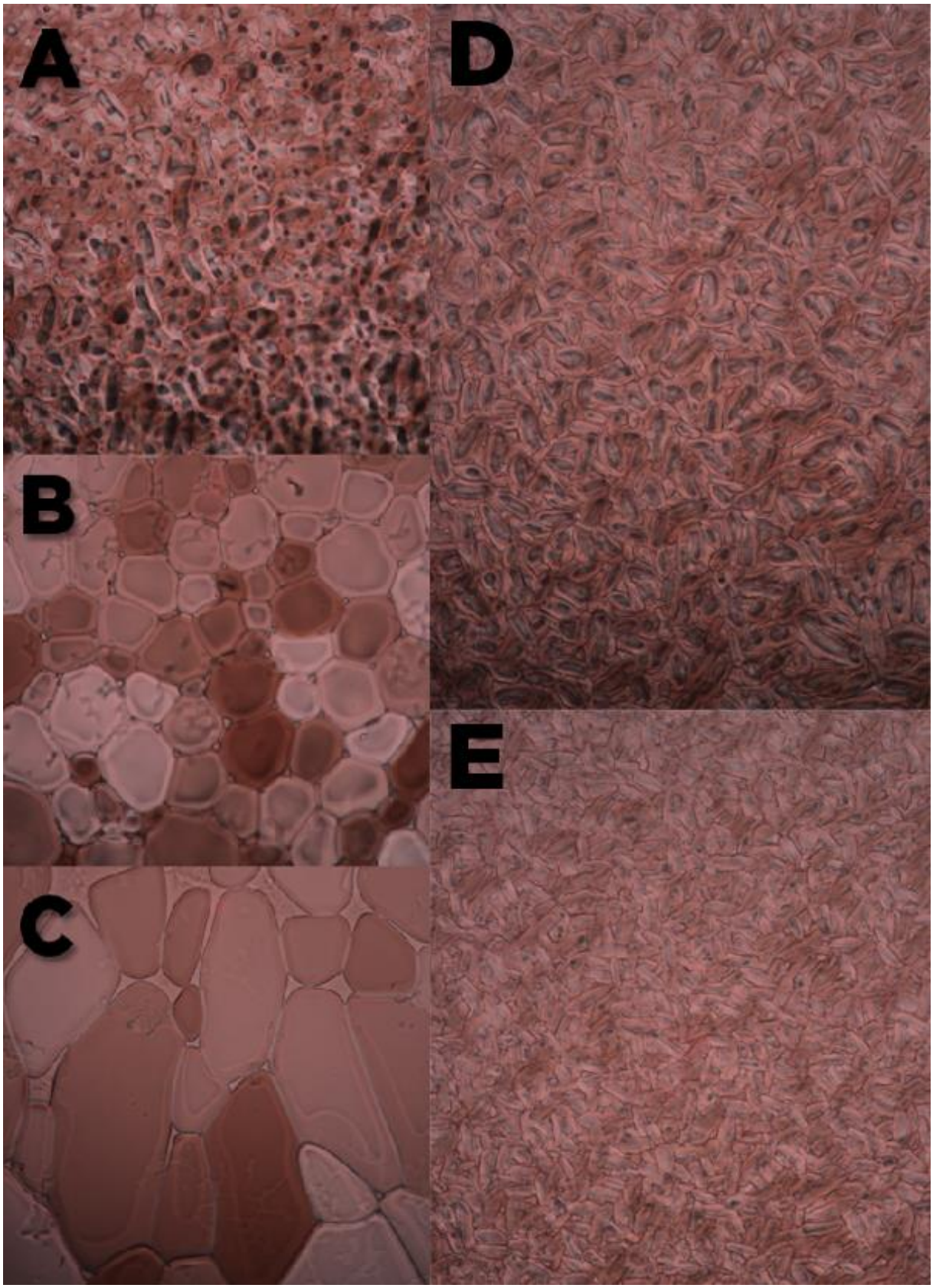

Figure 8 shows a series of pictures taken of the ice crystals at different times. A, B, C are each pictures of crystals grown in pure PBS solution, whilst D and E show pictures of crystal grown in 13kDa PVA 1 mg/ml solution. At A) t = 0 minutes, B) t = 30 minutes, C) t = 120 minutes, whereas D) t = 30 mins and E) t = 120 mins. Pcitures are taken at a 20x magnification.

inhibition is happening and so ice crystals cannot grow as fast. When compared directly as a percentage of the size of the average size of the crystal at a given time, we see that higher concentrations have lower percentages. This is because as the PBS crystals continue to grow with nothing retarding the ice crystal growth; they grow faster relative to the polymer samples and so the percentages all fall over time. Of course on top of this, the higher concentration crystals are growing slower than the lower concentrations, so this adds to the effect, hence why the 10 mg/ml sample has the lowest percentage after the full 2 hours.

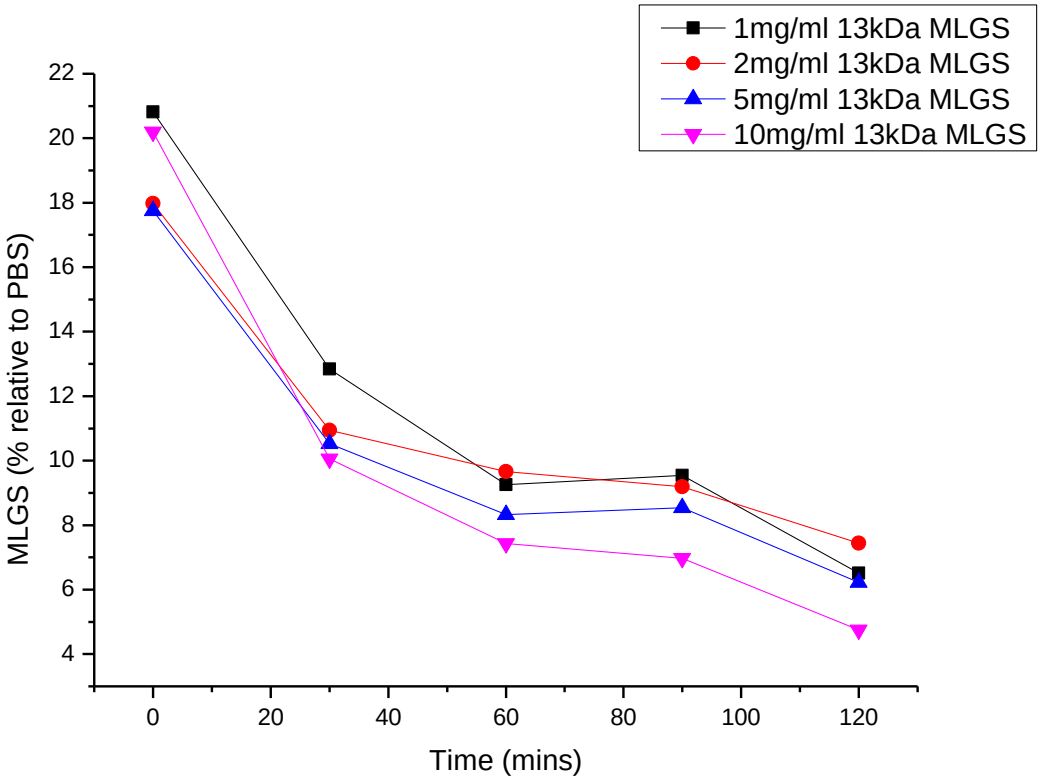

Figure 9 - A plot of the Mean Largest Grain Size of ice crystal in the polymer samples as a percentage of PBS crystal size as a function of time

One thing that has been noted is that at very high concentrations, polymer chains begin to micelle after reaching their respective critical micelle concentrations and which also means the polymers become increasingly difficult to dissolve and less soluble. As a result, there appears to be a slight loss of activity; however this is mostly negligible due to the sheer amount of PVA in solution. From Figure 9, shows what ice crystals actually look like in a splat test assay. Immediately it is clear the difference between when the polymer is present or not. With the polymer present there is next to no real growth over the 2 hour period, which

shows us that PVA is indeed active. It should also be mentioned lack of dynamic ice shaping into needle-like ice crystals suggests the PVA does not bind directly to the ice.

NMR Experiments

The spectra collected of the relaxation measurements, when processed, were phased and baseline corrected (to start at 0). Afterwards, the integrals of the water peaks were taken and plotted in origin along with the relevant fitting to extract the relaxation constant: T1 and T2. Typically T1 relaxation times correspond to fast motions whilst larger T2 values correspond to slower motions.

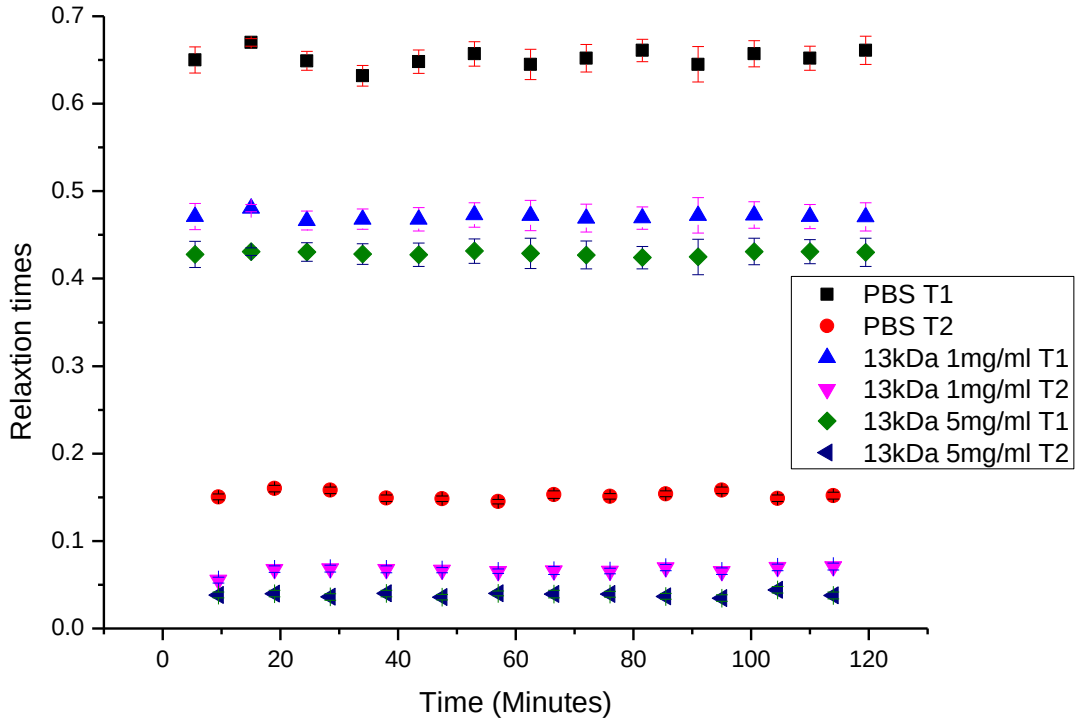

Figure 10 - Graph of Relaxation time meaurements taken over 2 hours one after the other (T1,T2,T1, etc)

As mentioned previously in the method, the initial idea was to run a series of NMR experiments over the same 2 hour period using the samples used in the splat test assay. This could mean that the mean largest grain sizes recorded from the splat test assays could be compared directly to relaxation times as a function of time. When running these relaxation experiments, the spectrometer was set up to continually run experiments one after the other via a batch list. By recording the time taken for each experiment to run, one could have plot a trend of relaxation times as the crystals grow as a function of time. The data could then be plotted against the Mean largest grain sizes to find additional trends. However, it was found

after performing these experiments and processing the spectra that on the whole the T1 and T2 relaxation times remain fairly constant throughout. Figure 10 shows a plot of the relaxation times as a function of time when the measurements were taken. We see, apart from a few mild fluctuations, that the relaxation time remains constant. This to an extent is to be expected seeing as the nmr signal measures the spins of all the protons in the sample and so is effectively measuring the bulk water. On average it this means things will stay relatively the same since with the sample is annealing at -8C, in the case of PBS, the water will be shifting to the thermodynamically favourable larger ice crystals, but at the same time overall water will be constantly thawing and refreezing.

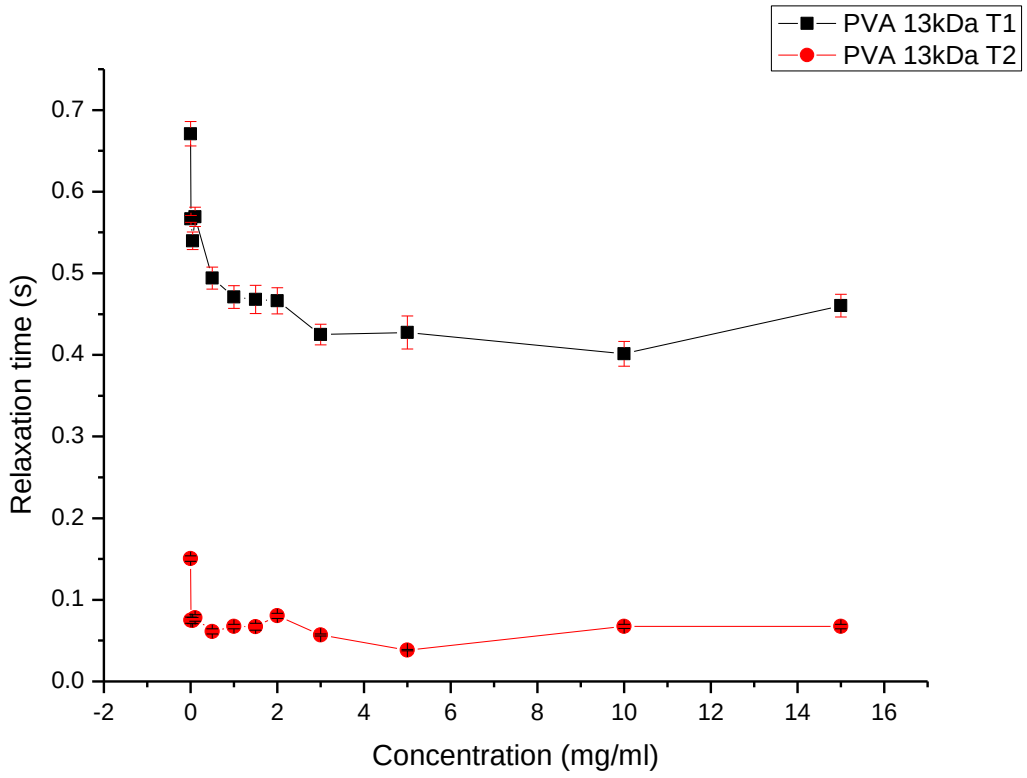

Figure 11 - Relaxation times of different 13kDa concentration samples

It was decided because of this, another approach to would be to try a multitude of samples and seeing what happens to the trend when changing 1 characteristic each time. Initially several different concentrations of 13kDa PVA were made up and T1 and T2 measurements carried out. As we see from the graph the general trend shows that the relaxation time fall as the concentration increases. The change in relaxation time can be related to the PVAs ability to interact with the ice lattice in some form or another. This is because of an increase in the overall intermolecular forces, Van de Waals playing a significant role. This increased

viscosity thus affects the tumbling rate of nuclei is solution since there is less freedom to do so even in the small amounts of unfrozen water expected to be in the hydration sphere around the polymer. This is to be expected for T1 times, since the viscosity of the solution changes, that is, increases as more polymer is dissolved into it.

It was mentioned earlier that the presence of hydroxyl groups is one characteristic that is believed to be necessary for effective IRI activity. With the addition of more polymer in solution there are more hydroxyl groups in solution on the polymer for them to interact with the ice. This is somewhat confirmed by the large difference between pure water (PBS) and solutions with polymer since some form of interaction must be taking place but this may not fully explain it. Something else that may be happening, is the polymer hydroxyl groups are interacting with thawed water constantly – such that they constantly hydrogen bond and unbond to water molecule, overall disordering the water and stopping it from freezing (becoming ordered due from being bound to the ice crystals). It's in this way that we can see that the grain sizes are effectively held in stasis unable to grow and the effect being increasingly more prominent the higher the concentration goes, to an extent. If we look at the times beyond 5 mg/ml, this is at the point where to the solution is becoming very viscous and also the point where the PVA begins to micelle and so we see a slight inversion of the trend. Similarly the T2 values are indicative of this, since they are quite low especially past the 3 mg/ml mark, which is indicative of stronger interactions between the water and polymer.

Similar trends are seen for 4.4kDa and 1kDa PVA as can be seen from Figure 12.

Overall though we see the main region where we see clearly activity and the increasing in activity is 5mg/ml and below.

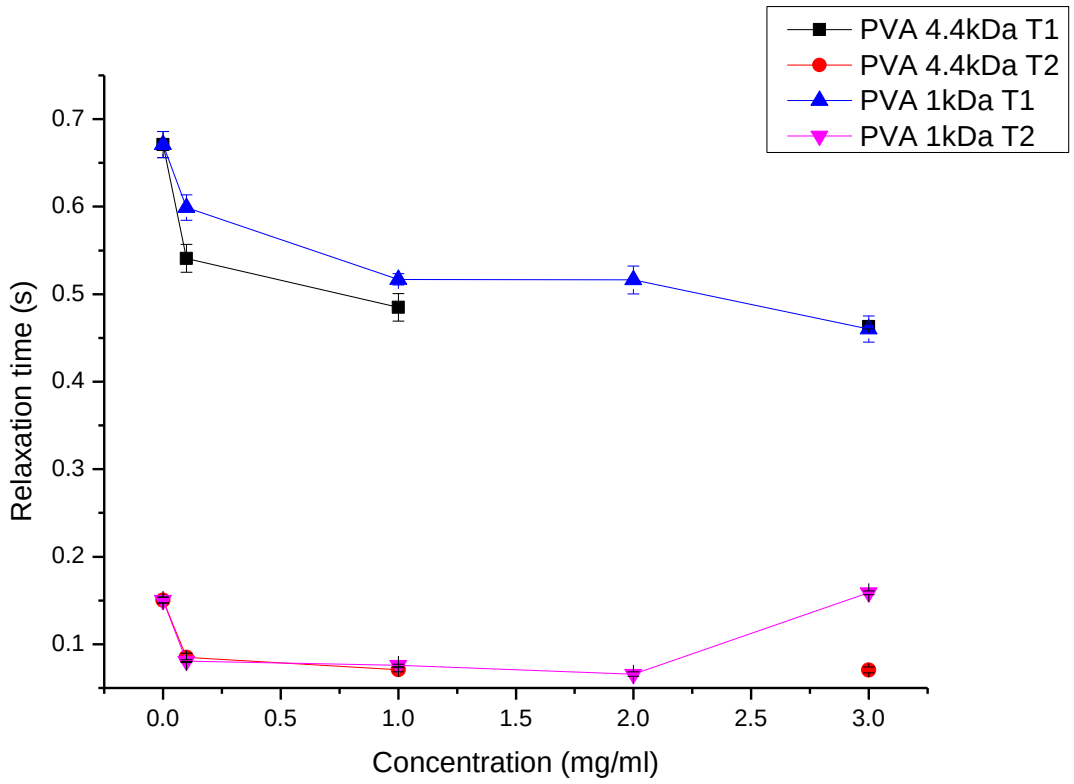

Figure 12 - Relaxation times for 4.4 kDa and 1 kDa PVA, also tested at numerous concentrations

Viscosity of Samples

Viscosities of the samples potentially have a critical role with regards to the relaxation times for the polymer solutions especially with the T1s. As discussed earlier, larger molecules and viscous solutions have longer spin-lattice relaxation time but shorter spin-spin relaxation times.

Kinematic viscosity is the ratio of absolute or dynamic viscosity to density - a quantity in which no force is involved. Kinematic viscosity can be obtained by dividing the absolute viscosity of a fluid with its mass density. In this particular case, the kinematic viscosities were taken from literature[25]:

Table 3 - Table of kinematic viscosities of PVA and PEG

Polymer	Equivalent concentration	Kinematic viscosity /cm^2s^{-1}
Water	n/a	0.68
0.1% PEG 400 Da	1 mg/ml 0.4 kDa	0.73
0.1% PEG 1400 Da	1 mg/ml 1.4 kDa	0.73
0.1% PEG 8000 Da	1 mg/ml 8 kDa	0.73
0.1% PEG 15000 Da	1 mg/ml 15 kDa	0.74
0.1% PVA 10000 Da	1 mg/ml 10 kDa	0.75
0.2% PEG 8000 Da	2 mg/ml 8 kDa	0.77
0.2% PVA 10000 Da	2 mg/ml 10 kDa	0.77

Intrinsic viscosity [η] is a measure of a solute's contribution to the viscosity of a solution. The intrinsic viscosity of both PEG and PVA can be worked out by using the Mark-Houwink equation and inputting the appropriate parameters:

$$[\eta] = KM^{\alpha}$$

Where K and α are constants specific to a solvent-solute pair.

From this equation the intrinsic viscosity can be worked out by the molecular weight of a polymer and databook values* of the K and α constants.

The constants for for PVA and PEG at 30C are:

Table 4 - Table of Mark-Houwink parameters for PVA and PEG at 30C

Polymer	α	K value	Intrinsic viscosity [η] dl/ g
PEG	0.57	0.0010400	0.575
PVA	0.64	0.000666	0.644

From the kinematic viscosities, we see the viscosities are close to each other on the whole, but the PVA has a slightly higher viscosity. This is also evident from the intrinsic viscosities.

As mentioned earlier viscosities effect the T1 values do to the slowing of tumbling rate. To account for this PEG samples were run.
PEG was used as a negative control for comparison of results with PVA in these experiments.

PEG has shown very low IRI activity in assay tests despite being an isomer of PVA. This gives further evidence that a pendent hydroxyl group is needed for good IRI activity on top of the ability to form hydrogen bonds.

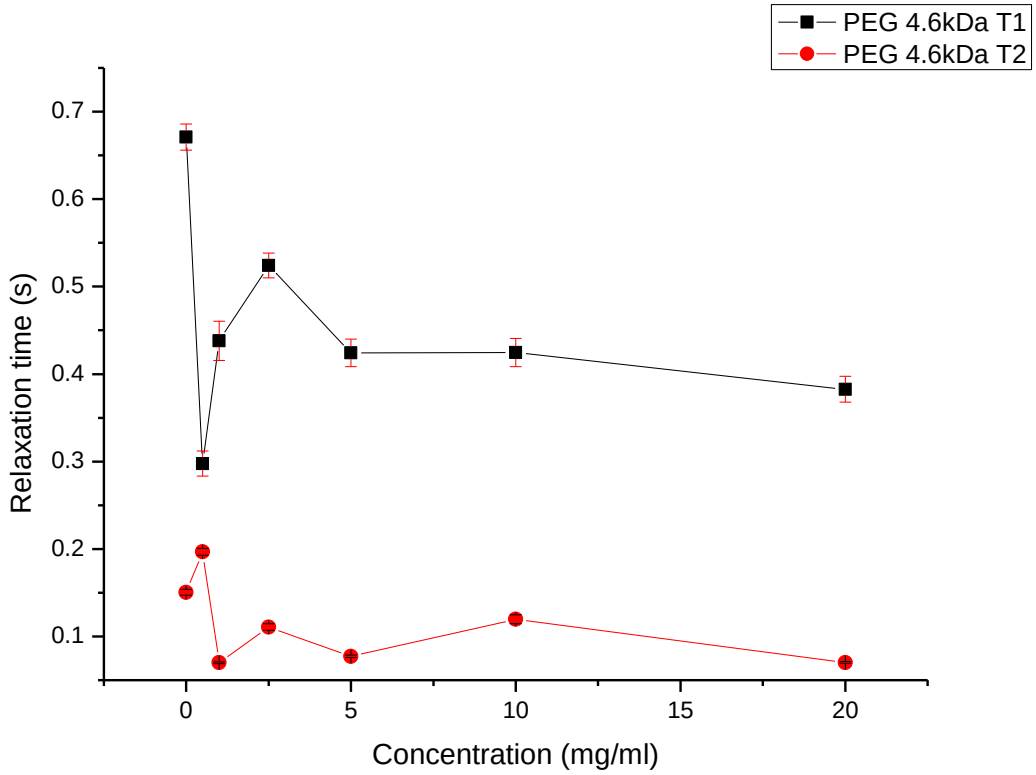

Figure 13 - Relaxations times of PEG 4.6 kDa

What we see here however is quite interesting. The PEG seems to show quite a different behaviour at lower concentrations but the T1s seem to correlate slightly at higher concentrations. What is quite peculiar, however, is the trend in relaxation times at lower concentrations. The sudden drop, if lower relaxation times were indicative of IRI activity as the PVA seems to suggest, would imply that PEG would show good activity at v. low temperatures. However, splat test assays have shown that this simply not the case. One thing that is evident though, is that overall, PVA shows lower T2 relaxation times: typically below 100 ms whilst the PEG seems to be 100 ms+. This again is indicative of contribution to some form of exchange process which can in turn indicate stronger interactions of the water molecules with some part of the polymer.

Conclusion

The study of ice crystals with the addition of cryoprotectants under solid-state NMR at low temperatures can be employed to investigate interaction between the ice and the cryoprotectant.

In the NMR experiments performed in this project, the T1 and T2 relxation times were used as indicators on whether the PolyVinylAlcohol and PolyEthylene Glycol did interact with the ice crystal lattice. Comparison of data with Ice crystal assays was also undertaken to show convincing data that the PVA does in fact prevent ice recrystallization growth. What was found is that there is evidence within the relaxation times, which tells us the PVA interacts with the ice crystals.

There is much future work that could be carried out to further this research. One thing that could be done is a series of experiments using deuterated PBS solution to measure distinctive quadrupolar relaxations. The differences in the strength of hydrogen bonding could reveal new information about PVAs IRI mechanism. A series of 2D exchange spectra could be undertaken to see what is actually interacting with what within the frozen solution.